PHYSICAL REVIEW D **91,** 054026 (2015)

# Valence quark distributions of the proton from maximum entropy approach

Rong Wang[1,2,3,*] and Xurong Chen[1]

[1]*Institute of Modern Physics, Chinese Academy of Sciences, Lanzhou 730000, China*
[2]*Lanzhou University, Lanzhou 730000, China*
[3]*University of Chinese Academy of Sciences, Beijing 100049, China*

(Received 14 October 2014; published 23 March 2015)

We present an attempt using the maximum entropy principle to determine valence quark distributions in the proton at a very low resolution scale $Q_0^2$. The initial three valence quark distributions are obtained with limited dynamical information from quark model and QCD theory. Valence quark distributions from this method are compared to the lepton deep inelastic scattering data, and the widely used CT10 and MSTW08 data sets. The obtained valence quark distributions are consistent with experimental observations and the latest global fits of parton distribution functions. The maximum entropy method is expected to be particularly useful in cases where relatively little information from QCD theory is given.

DOI: 10.1103/PhysRevD.91.054026 PACS numbers: 12.38.-t, 13.15.+g, 13.60.Hb, 14.20.Dh

## I. INTRODUCTION

Determination of parton distribution functions (PDFs) of the proton is of high interest in high energy physics [1–5], as PDFs are an essential tool for standard model phenomenology, theoretical prediction study, and some new physics searches. In perturbative quantum chromodynamics (QCD) theory, factorization allows for the computation of the hard partonic scattering processes involving initial hadrons, which requires the knowledge of the PDFs in the nucleon. The widely used PDFs are extracted from a global QCD analysis of experimental data on deep inelastic scattering (DIS), Drell-Yan, and jet production processes. The initial parton distributions at low scale $Q_0^2$ are called the nonperturbative input. Valence quarks form the main part of the nonperturbative input, for they carry most of the momentum of the proton. In the global analysis, the nonperturbative input is parametrized and evolved to high $Q^2$ to fit with the experimental measurements.

To date, the nonperturbative input has not been calculated in theory due to the complexity of nonperturbative QCD. However, there are many calculations of valence quark distributions from models, such as the MIT bag model [6,7] and the Nambu– Jona-Lasinio model [8]. These model-calculated valence quark distributions in the nucleon are in agreement with the global analysis. Determination of the nonperturbative input apart from the global fit procedure is not only a complement to a current extraction of PDFs, but also helps us understand the structure and the nature of the hadrons. In addition, a precise determination of valence quark distributions is important for the detailed study of sea quarks in the intermediate $x$ region [9].

In this article, we try to determine the valence quark distributions of the proton using the maximum entropy method, based on some already known structural information and properties of the proton in the naive quark model and QCD theory. The maximum entropy principle is a rule for converting certain types of information, called testable information, to a probability assignment [10–13]. In this analysis, the known properties of the proton are the testable information, and the valence quark distributions are the probability density functions that need to be assigned. The maximum entropy method gives the least biased estimate possible on the given information. It is widely used in lattice QCD (LQCD) [14,15], with reliable results and high efficiency.

The organization of the paper is as follows. A naive nonperturbative input is introduced in Sec. II. Section III discusses the standard deviations of parton momentum distributions, which are related to quark confinement and the Heisenberg uncertainty principle. In Sec. IV, the maximum entropy method is demonstrated. Section V presents comparisons of our results with experimental data and the global analysis results. Finally, discussions and a summary are given in Sec. VI.

## II. A NAIVE NONPERTURBATIVE INPUT FROM THE QUARK MODEL

The quark model is very successful in the hadron spectroscopy study and in describing the reaction dynamics. The quark model is based on some basic symmetries which uncover some important inner structures of the hadrons. The proton consists of a complex mixture of quarks and gluons in hard scattering processes at high $Q^2$. In view of the quark model, the origin of the PDFs is the three valence quarks. In the dynamical PDF model, the sea quarks and gluons are radiatively generated from three dominated valence quarks and "valencelike" components which are of small quantities [4,16,17].

The solutions of the QCD evolution equations for parton distributions at high $Q^2$ depend on the initial parton

*rwang@impcas.ac.cn

 

distributions at low $Q_0^2$. An ideal assumption is that the proton consists of only valence quarks at extremely low $Q_0^2$. Thus, a naive nonperturbative input of the proton includes merely three valence quarks [18–21], which is the simplest initial parton distribution. All sea quarks and gluons at high $Q^2$ ($> Q_0^2$) are dynamically produced from the QCD evolution. In fact, there are other types of sea quarks at the starting scale, such as intrinsic sea [22,23], connected sea [24–26] and cloud sea [27–29]. Nonetheless, the naive nonperturbative input is generally a good approximation because other origins of sea quarks are of small contributions. The naive nonperturbative input with three valence quarks is very natural in the quark model.

In our analysis, valence quark distribution functions at $Q_0^2$ are parametrized to approximate the analytical solution of nonperturbative QCD. The simplest function form to approximate valence quark distribution is the time-honored canonical parametrization $f(x) = Ax^B(1-x)^C$ [1]. Hence, the simplest parametrization of the naive nonperturbative input is written as

$$u_v(x, Q_0^2) = A_u x^{B_u}(1-x)^{C_u}, d_v(x, Q_0^2) = A_d x^{B_d}(1-x)^{C_d}. \tag{1}$$

The parametrization above has poles at $x = 0$ and $x = 1$ to represent the singularities associated with Regge behavior at small $x$ and quark counting rules at large $x$.

In the quark model, the proton has two up valence quarks and one down valence quark. Therefore, we have the valence sum rules for the naive nonperturbative input

$$\int_0^1 u_v(x, Q_0^2)dx = 2, \qquad \int_0^1 d_v(x, Q_0^2)dx = 1. \tag{2}$$

Since there are no sea quarks and gluons in the naive nonperturbative input, valence quarks take the total momentum of the proton. We have the momentum sum rule for valence quarks at $Q_0^2$,

$$\int_0^1 x[u_v(x, Q_0^2) + d_v(x, Q_0^2)]dx = 1. \tag{3}$$

## III. STANDARD DEVIATIONS OF QUARK DISTRIBUTION FUNCTIONS

The confinement of quarks is a basic feature in non-Abelian gauge field theory [30]. Phenomenologically, Cornell potential is successful for describing heavy quarkonium, which has linear potential at a large distance [31,32]. The linear potential is also realized in LQCD [33,34]. In the MIT bag model [35–37], fields are confined to a finite region of space. Without a doubt, valence quarks inside a proton are confined in a small space region.

According to the Heisenberg uncertainty principle, the momenta of quarks in the proton are uncertain, which have the probability density distributions. The Heisenberg uncertainty principle is

$$\sigma_X \sigma_P \geq \frac{\hbar}{2}. \tag{4}$$

To avoid misidentification, the capital $X$ in the above formula denotes the ordinary space coordinate, as the lowercase $x$ already denotes the Bjorken scaling variable. $P$ denotes the momentum in $X$ direction. $\sigma_X$ is the standard deviation of the spacial position of one parton in the $X$ direction and $\sigma_P$, accordingly, is the standard deviation of momentum. In quantum mechanics, the uncertainty relation is $\sigma_X\sigma_P = 0.568\hbar$ for a particle in a one-dimensional box, and $\sigma_X\sigma_P = \hbar/2$ for the quantum harmonic oscillator at the ground state. In order to constrain the standard deviations of quark momentum distributions, $\sigma_X\sigma_P = \hbar/2$ is taken for the three initial valence quarks in our analysis instead of $\sigma_X\sigma_P \geq \hbar/2$.

$\sigma_X$ is related to the radius of the proton. A simple estimation is to transform the sphere proton into a cylinder proton, which gives $\sigma_X = (2\pi R^3/3)/(\pi R^2) = 2R/3$, with $R = \sqrt{\langle r_p^2 \rangle}$ being the charge radius of the proton. The proton charge radius is precisely measured in muonic hydrogen Lamb shift experiments, which is obtained as 0.841 fm [38,39]. $\sigma_X$ of each up valence quark is divided by $2^{1/3}$, for there are two up valence quarks sharing the same space region. The confinement space region for the up valence quark is half of the total confinement space. This is an assumption we proposed, not the Pauli blocking principle. The two up valence quarks have positive electric charges; therefore, it is very hard for them to approach each other closely. Consequently, we have $\sigma_{X_d} = 2R/3$ and $\sigma_{X_u} = 2R/(3 \times 2^{1/3})$.

The Bjorken variable $x$ is the momentum fraction one parton takes from the proton momentum in the quark parton model. Therefore, we define the standard deviation of $x$ at the extremely low resolution scale $Q_0^2$ as

$$\sigma_x = \frac{\sigma_P}{M_p}. \tag{5}$$

$M_p$ is the mass of the proton, which is 0.938 GeV [40]. The natural unit is used in all of the calculations of this work. Finally, constraints for valence quark distributions from QCD confinement and the Heisenberg uncertainty principle are expressed as follows:

$$\begin{aligned}
&\sqrt{\langle x_u^2 \rangle - \langle x_u \rangle^2} = \sigma_{x_u}, \qquad \sqrt{\langle x_d^2 \rangle - \langle x_d \rangle^2} = \sigma_{x_d}, \\
&\langle x_u \rangle = \int_0^1 x \frac{u_v(x, Q_0^2)}{2} dx, \qquad \langle x_d \rangle = \int_0^1 x d_v(x, Q_0^2)dx, \\
&\langle x_u^2 \rangle = \int_0^1 x^2 \frac{u_v(x, Q_0^2)}{2} dx, \qquad \langle x_d^2 \rangle = \int_0^1 x^2 d_v(x, Q_0^2)dx.
\end{aligned} \tag{6}$$

## IV. MAXIMUM ENTROPY METHOD

From the above analysis, we do know a lot of information about the valence quark distributions, but we still

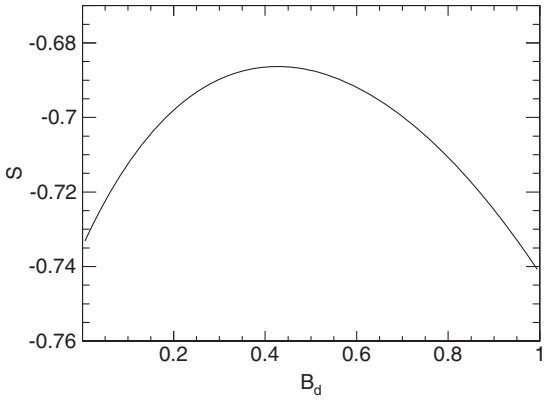


FIG. 1. Information entropy $S$ is plotted as a function of the parameter $B_d$.

cannot get the exact distributions. By applying the maximum entropy principle, we can find the most reasonable valence quark distributions from the testable information, which are the constraints discussed above. The generalized information entropy of valence quarks is defined as

$$S = -\int_0^1 \left[ 2\frac{u_v(x,Q_0^2)}{2} \ln\left(\frac{u_v(x,Q_0^2)}{2}\right) + d_v(x,Q_0^2)\ln(d_v(x,Q_0^2)) \right] dx. \quad (7)$$

The best estimated nonperturbative input will have the largest entropy. Valence quark distributions are assigned by taking the maximum entropy.

With the constraints given by Eqs. (2), (3), and (6), there is only one free parameter left for the parametrized naive nonperturbative input. We take $B_d$ as the only free parameter. Figure 1 shows the information entropy of valence quark distributions of the proton at the starting scale as a function of the parameter $B_d$. By taking the maximum of the entropy, $B_d$ is optimized as 0.427. The corresponding valence quark distributions are

$$u_v(x,Q_0^2) = 4.589x^{0.095}(1-x)^{1.000},$$
$$d_v(x,Q_0^2) = 7.180x^{0.427}(1-x)^{2.456}. \quad (8)$$

## V. RESULTS

By performing Dokshitzer-Gribov-Lipatov-Altarelli-Parisi (DGLAP) evolution [41–43], we can determine valence quark distributions at high scale with the input obtained in Eq. (8). There are only three valence quarks in the proton. Higher twist corrections to the DGLAP equation for valence evolution are small, for the density of the valence quark is not big. With the DGLAP equation, the obtained naive nonperturbative input can be tested with the experimental measurements at high $Q^2$. In this work, we use leading order (LO) and next-to-next-to-leading order (NNLO) evolution. We get the specific starting scale $Q_0^2 = 0.064\ \mathrm{GeV}^2$ for the LO evolution (with $\Lambda_{\mathrm{QCD}} = 0.204$ GeV for $f = 3$ flavors) by using QCD evolution for the second moments of the valence quark distributions [44] and the measured moments of the valence quark distributions at a higher $Q^2$ [4]. This energy scale is very close to the starting scale for bag model PDFs, which is $0.0676\ \mathrm{GeV}^2$ [6]. The running coupling constant $\alpha_s$ and the quark masses are the fundamental parameters of perturbative QCD. The running coupling constant for the LO evolution we choose is

$$\frac{\alpha_s(Q^2)}{4\pi} = \frac{1}{\beta_0 \ln(Q^2/\Lambda^2)}, \quad (9)$$

in which $\beta_0 = 11 - 2f/3$ and $\Lambda_{\mathrm{LO}}^{3,4,5,6} = 204, 175, 132, 66.5$ MeV [4]. For the $\alpha_s$ matchings, we take $m_c = 1.4$ GeV, $m_b = 4.5$ GeV, $m_t = 175$ GeV for the LO evolution. For the NNLO DGLAP evolution, we use the modified Mellin transformation method by CANDIA [45], with $\alpha_s(M_z^2) = 0.1155$ and $m_c = 1.43$ GeV, $m_b = 4.3$ GeV, $m_t = 175$ GeV. The starting scale for the NNLO evolution we choose is $Q_0^2 = 0.22\ \mathrm{GeV}^2$, which is close to $\Lambda_{f=3,\mathrm{NNLO}}^2 = 0.2\ \mathrm{GeV}^2$. In the NNLO evolution, we have $\alpha_s(Q_0^2)/(2\pi) = 0.3$.

The isoscalar structure function $xF_3$ from neutrino and antineutrino scattering data provides valuable information of valence quark distributions. The connection between $xF_3$ and the valence quark distributions is given by $xF_3(x,Q^2) = xu_v(x,Q^2) + xd_v(x,Q^2)$. Our predicted $xF_3$ as a function of $x$ at high $Q^2$ is shown in Fig. 2, compared with results from the NuTeV and CCFR experiments. The predicted $xF_3$ is in excellent agreement with the experimental data in the large $x$ region ($x > 0.3$). On the whole, the LO and NNLO results are consistent with

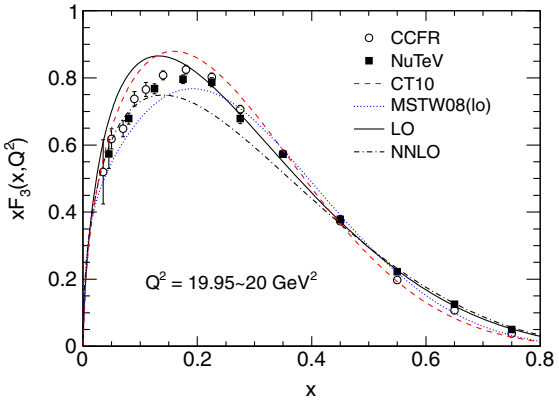


FIG. 2 (color online). Comparisons of our predicted structure function $xF_3$ (solid and dot-dashed lines) with experimental data from NuTeV (squares) [46] and CCFR (open circles) [47]. Only statistical errors of the experimental data are plotted. Results of CT10 (dashed line) [2] and MSTW08(LO) (dotted line) [3] from a global fit are also shown here.

the experiments except for a small discrepancy around $x = 0.1$ and around $x = 0.2$, respectively. CT10 and MSTW08 (LO) data sets of the QCD global analysis are also plotted in the figure. Our predicted $xF_3$ is close to that of CT10 and MSTW08(LO).

Structure function $F_2$ plays quite a significant role in determining PDFs, for it is related to quark distributions directly. As we know, valence quarks dominate in the large $x$ region. Therefore, $F_2$ at large $x$ is mainly from contributions of valence quarks. By assuming that there are no sea quarks at $x \geq 0.4$, the calculated $F_2$'s as a function of $Q^2$ are shown in Fig. 3, compared with the recent results from HERA [48]. Basically, our predicted $F_2$'s are consistent with the $e^{\pm}p$ neutral-current DIS data.

Structure function ratio $F_2^n/F_2^p$ is sensitive to both up and down quark distributions. In the large $x$ region, it is mainly related to the up and down valence quark distributions. Under the assumption of isospin symmetry between the proton and the neutron, up valence quark distribution in the proton is identical with down valence quark distribution in the neutron. Figure 4 shows the predicted structure function ratios $F_2^n/F_2^p$ from valence contribution only. Sea quarks are ignored in the calculation. Experimental results from NMC [49] and Arrington *et al.* [50] are also shown in the figure. Data from Arrington *et al.* represent a detailed analysis of previous experimental data within the framework of relativistic quantum mechanics for the deuteron structure. Our results are in excellent agreement with the experimental data in the large $x$ region.

Up and down valence quark ratios $d_v/u_v$ are extracted in neutrino DIS and charged $\pi$ semi-inclusive DIS processes.

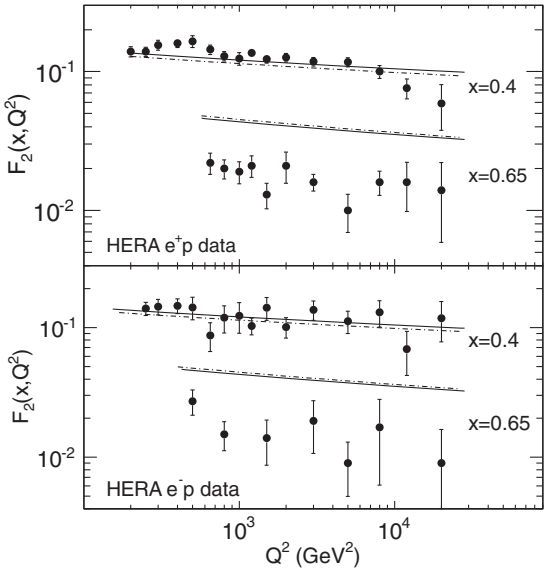


FIG. 3. Solid lines and dot-dashed lines are LO and NNLO predictions, respectively. The combined HERA data [48] are shown in circles. Errors shown in the figure are the total experimental uncertainties. Our predicted $F_2$'s are from valence contribution only, assuming sea quarks are negligible at large $x$.

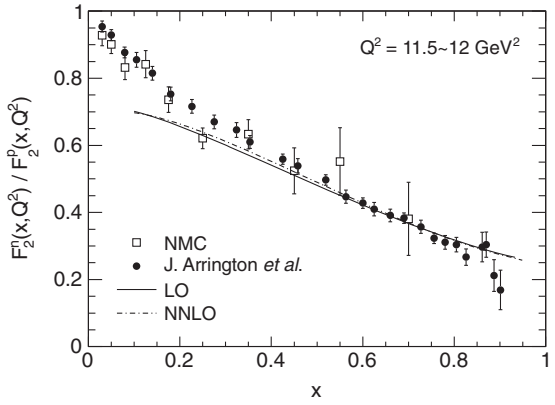


FIG. 4. The predicted $F_2$ ratios of neutron to proton (solid and dot-dashed lines) are shown with the experimental data. Our predicted $F_2$ ratios are calculated without the contributions of sea quarks. NMC data (open squares) is taken from [49]. Detailed analysis data (circles) [50] is from Arrington *et al*. The plotted errors of experimental data are the total uncertainties.

Our predicted $d_v/u_v$ ratios are shown in Fig. 5 with experimental results from CDHS [51], WA21 [52], and HERMES [53]. Predicted $d_v/u_v$ ratios at $Q^2 = 4$ GeV$^2$ are plotted in the figure. $d_v/u_v$ ratios have weak $Q^2$ dependence. The predicted $d_v/u_v$ ratios agree well with the experimental data.

Figure 6 shows the comparisons of our predicted up and down valence quark momentum distributions, multiplied by $x$, at $Q^2 = 10$ GeV$^2$ with the global fits from CT10 [2] and MSTW08(LO) [3]. In general, our obtained up and down valence quark momentum distributions are consistent with the popular parton distribution functions from QCD global analysis.

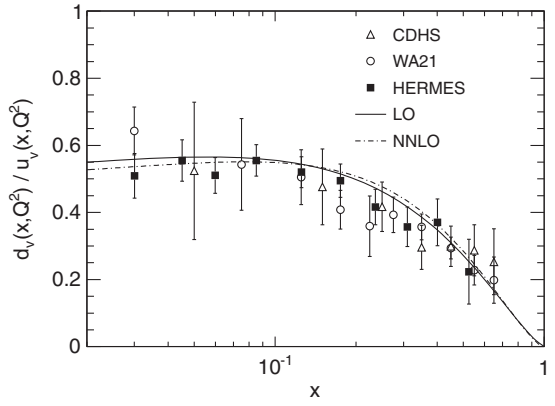


FIG. 5. Comparisons of our predicted $d_v/u_v$ ratios (solid and dot-dashed lines) with experimental results from CDHS (open triangle) [51], WA21 (open circle) [52], and HERMES (squares) [53]. The plotted errors are the total errors. Our predicted ratios are at $Q^2 = 4$ GeV$^2$. HERMES data is at mean $Q^2 = 2.4$ GeV$^2$. $Q^2$ of the CDHS data varies from 3.3 to 42.9 GeV$^2$; $Q^2$ of the WA21 data varies from 3.4 to 36.5 GeV$^2$.

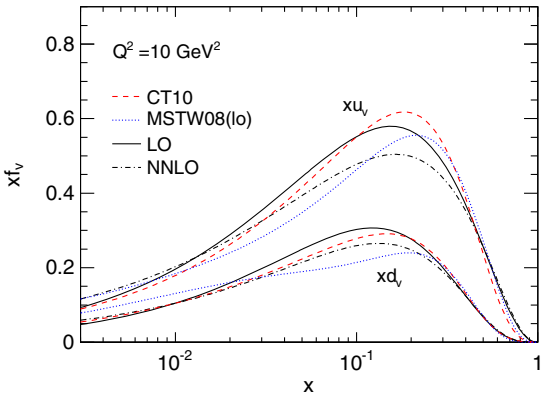


FIG. 6 (color online). Comparisons of our predicted valence quark momentum distributions (solid and dot-dashed lines) with global QCD fit CT10 (dashed lines) [2] and MSTW08(LO) (dotted lines) [3].

## VI. DISCUSSIONS AND SUMMARY

Valence quark distributions are given using the maximum entropy method. This is an interesting attempt to determine the parton distribution functions using a new method instead of the conventional global fit. The obtained valence quark distributions are consistent with the experimental observations from the high energy lepton probe and PDFs from global analysis. The determined valence quark distributions are reasonable and can be used for making theoretical predictions. Furthermore, if we make a more complicated parametrization for the nonperturbative input and include more constraints, the result possibly gets better. The Gross– Llewellyn Smith sum rule [54–56] could be the further constraint which would provide more information on valence quark distributions at high $Q^2$. The Ellis-Jaffe sum rule [57,58] could be practically useful to constrain the polarized PDFs.

Determining valence quark distributions from the maximum entropy method helps us to understand the primary aspects of the nucleon structure and to search for more details of the nucleon. First, our analysis shows that the origin of PDFs at high $Q^2$ is mainly the three valence quarks. A simple and naive nonperturbative input is introduced, and obtained, though it is just an approximation of the complex proton. Second, the basic features of valence quark distributions are related to the classic quark model assumption, the radius of the proton, and the mass of the proton. Third, the equation of the uncertainty relation for valence quarks is taken to be the relation for the quantum harmonic oscillator at the ground state. The uncertainty of the momentum could be a little larger. With the uncertainty being 10% larger, the obtained prediction becomes a little worse compared to the experiments. A more detailed study of the confinement potential will put on more accurate constraints to the uncertainty relation. Finally, the time-honored canonical parametrization scheme for valence quarks is very simple, but acceptable.

The maximum entropy method is applicable for obtaining details of interest with the least bias in situations where detailed information is not given. It is difficult to calculate the radius and the mass of the proton from nonperturbative QCD. LQCD has not acquired the detailed information of nucleon structure so far. However, we do know the radius and the mass of the proton from measurements in experiments and the confinement of quarks in QCD theory. With these experimental observations and some assumptions, the best estimates of valence quark distributions are obtained from the maximum entropy method. Because of its simplicity, this method can be easily applied to other types of PDFs, such as polarized PDFs, generalized parton distributions, and transverse momentum dependent PDFs. The maximum entropy method is particularly useful for digging reasonable results in situations where relatively little information from QCD calculations is given.

## ACKNOWLEDGMENTS

This work was supported by the National Basic Research Program of China (the 973 Program) under Grant No. 2014CB845406, the National Natural Science Foundation of China under Grant No. 11175220, and the Century Program of the Chinese Academy of Sciences under Grant No. Y101020BR0.

[1] J. Pumplin, D. R. Stump, J. Huston, H.-L. Lai, P. Nadolsky, and W.-K. Tung, J. High Energy Phys. 07 (2002) 012.
[2] H.-L. Lai, M. Guzzi, J. Huston, Z. Li, P. M. Nadolsky, J. Pumplin, and C.-P. Yuan, Phys. Rev. D **82**, 074024 (2010).
[3] A. D. Martin, W. J. Stirling, R. S. Thorne, and G. Watt, Eur. Phys. J. C **63**, 189 (2009).
[4] M. Glück, E. Reya, and A. Vogt, Eur. Phys. J. C **5**, 461 (1998).
[5] S. Alekhin, J. Blümlein, and S. Moch, Phys. Rev. D **86**, 054009 (2012).
[6] F. M. Steffens and A. W. Thomas, Prog. Theor. Phys. Suppl. **120**, 145 (1995).
[7] R. J. Holt and C. D. Roberts, Rev. Mod. Phys. **82**, 2991 (2010).
[8] H. Mineo, W. Bentz, N. Ishii, A. W. Thomas, and K. Yazaki, Nucl. Phys. **A735**, 482 (2004).

[9] J.-C. Peng, W.-C. Chang, H.-Y. Cheng, T.-J. Hou, K.-F. Liu, and J.-W. Qiu, Phys. Lett. B **736**, 411 (2014).
[10] E. T. Jaynes, Phys. Rev. **106**, 620 (1957).
[11] E. T. Jaynes, Phys. Rev. **108**, 171 (1957).
[12] A. Caticha, arXiv:0808.0012.
[13] U. von Toussaint, Rev. Mod. Phys. **83**, 943 (2011).
[14] M. Asakawa, Y. Nakaharat, and T. Hatsuda, Prog. Part. Nucl. Phys. **46**, 459 (2001).
[15] H.-T. Ding, A. Francis, O. Kaczmarek, F. Karsch, H. Satz, and W. Söldner, J. Phys. G **38**, 124070 (2011).
[16] A. Vogt, Phys. Lett. B **354**, 145 (1995).
[17] P. Jimenez-Delgado and E. Reya, Phys. Rev. D **79**, 074023 (2009).
[18] G. Parisi and R. Petronzio, Phys. Lett. **62B**, 331 (1976).
[19] A. I. Vainshtein, V. I. Zakharov, V. A. Novikov, and M. A. Shifman, JETP Lett. **24**, 341 (1976).
[20] M. Glück and E. Reya, Nucl. Phys. **B130**, 76 (1977).
[21] X. Chen, J. Ruan, R. Wang, P. Zhang, and W. Zhu, Int. J. Mod. Phys. E **23**, 1450057 (2014).
[22] S. J. Brodsky, P. Hoyer, C. Peterson, and N. Sakai, Phys. Lett. **93B**, 451 (1980).
[23] W.-C. Chang and J.-C. Peng, Phys. Rev. Lett. **106**, 252002 (2011).
[24] K.-F. Liu and S.-J. Dong, Phys. Rev. Lett. **72**, 1790 (1994).
[25] K.-F. Liu, Phys. Rev. D **62**, 074501 (2000).
[26] K.-F. Liu, W.-C. Chang, H.-Y. Cheng, and J.-C. Peng, Phys. Rev. Lett. **109**, 252002 (2012).
[27] A. Signal, A. W. Schreiber, and A. W. Thomas, Mod. Phys. Lett. A **06**, 271 (1991).
[28] W. Melnitchouk, J. Speth, and A. W. Thomas, Phys. Rev. D **59**, 014033 (1998).
[29] N. N. Nikolaev, W. Schäfer, A. Szczurek, and J. Speth, Phys. Rev. D **60**, 014004 (1999).
[30] K. G. Wilson, Phys. Rev. D **10**, 2445 (1974).
[31] E. Eichten, K. Gottfried, T. Kinoshita, J. B. Kogut, K. D. Lane, and T.-M. Yan, Phys. Rev. Lett. **34**, 369 (1975); **36**, 1276(E) (1976).
[32] E. Eichten, K. Gottfried, T. Kinoshita, K. D. Lane, and T.-M. Yan, Phys. Rev. D **17**, 3090 (1978); **21**, 313(E) (1980).
[33] T. Kawanai and S. Sasaki, Phys. Rev. D **85**, 091503(R) (2012).
[34] P. W. M. Evans, C. R. Allton, and J.-I. Skullerud, Phys. Rev. D **89**, 071502(R) (2014).
[35] A. Chodos, R. L. Jaffe, K. Johnson, C. B. Thorn, and V. F. Weisskopf, Phys. Rev. D **9**, 3471 (1974).
[36] A. Chodos, R. L. Jaffe, K. Johnson, and C. B. Thorn, Phys. Rev. D **10**, 2599 (1974).
[37] T. DeGrand, R. L. Jaffe, K. Johnson, and J. Kiskis, Phys. Rev. D **12**, 2060 (1975).
[38] R. Pohl *et al.*, Nature (London) **466**, 213 (2010).
[39] A. Antognini *et al.*, Science **339**, 417 (2013).
[40] K. A. Olive *et al.* (Particle Data Group), Chin. Phys. C **38**, 090001 (2014).
[41] Y. L. Dokshitzer, Sov. Phys. JETP **46**, 641 (1977).
[42] V. N. Gribov and L. N. Lipatov, Sov. J. Nucl. Phys. **15**, 438 (1972).
[43] G. Altarelli and G. Parisi, Nucl. Phys. **B126**, 298 (1977).
[44] G. Altarelli, Phys. Rep. **81**, 1 (1982).
[45] A. Cafarella, C. Corian, and M. Guzzi, Comput. Phys. Commun. **179**, 665 (2008).
[46] M. Tzanov *et al.*, Phys. Rev. D **74**, 012008 (2006).
[47] W. G. Seligman *et al.* (CCFR Collaboration), Phys. Rev. Lett. **79**, 1213 (1997).
[48] F. D. Aaron *et al.* (H1 and ZEUS Collaborations), J. High Energy Phys. 01 (2010) 109.
[49] P. Amaudruz *et al.* (NMC Collaboration), Nucl. Phys. **B371**, 3 (1992).
[50] J. Arrington, F. Coester, R. J. Holt, and T.-S. H. Lee, J. Phys. G **36**, 025005 (2009).
[51] H. Abramowicz *et al.* (CDHS Collaboration), Z. Phys. C **25**, 29 (1984).
[52] G. T. Jones *et al.* (WA21 Collaboration), Z. Phys. C **62**, 601 (1994).
[53] J. E. Belz *et al.* (HERMES Collaboration), *Proceedings of the 7th International Symposium on Meson-Nucleon Physics and the Structure of the Nucleon, Vancouver, Canada, 1997*, edited by D. Drechsel, G. Hohler, W. Kluge, H. Leutwyler, H. M. Staudenmaier, and B. M. K. Nefkens (TRIUMF, Vancouver, Canada, 1997).
[54] D. J. Gross and C. H. Llewellyn Smith, Nucl. Phys. **B14**, 337 (1969).
[55] S. A. Larin and J. A. M. Vermaseren, Phys. Lett. B **259**, 345 (1991).
[56] J. T. Londergan and A. W. Thomas, Phys. Rev. D **82**, 113001 (2010).
[57] J. Ellis and R. Jaffe, Phys. Rev. D **9**, 1444 (1974).
[58] A. L. Kataev, Phys. Rev. D **50**, R5469 (1994).